Sea-Level Highstand 81,000 Years Ago in Mallorca

Jeffrey A. Dorale, *et al.*

Science **327**, 860 (2010);
DOI: 10.1126/science.1181725

13. S. Raugei, M. L. Klein, *J. Chem. Phys.* **116**, 196 (2002).
14. C. Krekeler, B. Hess, L. Delle Site, *J. Chem. Phys.* **125**, 054305 (2006).
15. Materials and methods are available as supporting material on *Science* Online.
16. N. T. Hunt, A. A. Jaye, S. R. Meech, *Phys. Chem. Chem. Phys.* **9**, 2167 (2007).
17. G. D. Goodno, G. Dadusc, R. J. D. Miller, *J. Opt. Soc. Am. B* **15**, 1791 (1998).
18. S. Kano, M. D. Levenson, *Introduction to Nonlinear Laser Spectroscopy* (Oxford Univ. Press, New York, 1988).
19. S. Kinoshita, Y. Kai, M. Yamaguchi, T. Yagi, *Chem. Phys. Lett.* **236**, 259 (1995).
20. C. J. Fecko, J. D. Eaves, A. Tokmakoff, *J. Chem. Phys.* **117**, 1139 (2002).
21. D. Frenkel, J. P. McTague, *J. Chem. Phys.* **72**, 2801 (1980).
22. G. E. Walrafen, *J. Chem. Phys.* **40**, 3249 (1964).
23. I. Ohmine, S. Saito, *Acc. Chem. Res.* **32**, 741 (1999).
24. K. Mizoguchi, T. Ujike, Y. Tominaga, *J. Chem. Phys.* **109**, 1867 (1998).
25. P. Ayotte, G. H. Weddle, J. Kim, M. A. Johnson, *J. Am. Chem. Soc.* **120**, 12361 (1998).
26. D. J. Tobias, P. Jungwirth, M. Parrinello, *J. Chem. Phys.* **114**, 7036 (2001).
27. H. Ohtaki, T. Radnai, *Chem. Rev.* **93**, 1157 (1993).
28. C. D. Wick, S. S. Xantheas, *J. Phys. Chem. B* **113**, 4141 (2009).
29. We are grateful to the Engineering and Physical Sciences Research Council for financial support and to M. Kondo and V. Oganesyan for assistance with the DFT calculations.

Supporting Online Material
www.sciencemag.org/cgi/content/full/327/5967/857/DC1
Materials and Methods
Figs. S1 to S9
References

26 October 2009; accepted 8 December 2009
10.1126/science.1183799

Sea-Level Highstand 81,000 Years Ago in Mallorca

Jeffrey A. Dorale,[1]* Bogdan P. Onac,[2]* Joan J. Fornós,[3] Joaquin Ginés,[3] Angel Ginés,[3] Paola Tuccimei,[4] David W. Peate[1]

Global sea level and Earth's climate are closely linked. Using speleothem encrustations from coastal caves on the island of Mallorca, we determined that western Mediterranean relative sea level was ~1 meter above modern sea level ~81,000 years ago during marine isotope stage (MIS) 5a. Although our findings seemingly conflict with the eustatic sea-level curve of far-field sites, they corroborate an alternative view that MIS 5a was at least as ice-free as the present, and they challenge the prevailing view of MIS 5 sea-level history and certain facets of ice-age theory.

Large fluctuations in global sea level occurred throughout the last interglacial/glacial cycle, but the precise magnitudes of some of these fluctuations are subjects of energetic debate. The eustatic (ice equivalent) sea-level height of the marine isotope stage (MIS) 5a highstand event is among the more controversial of these sea-level variations, with estimates ranging widely from +3 to –30 m relative to modern sea level (*1*–*6*). Along the coast of Mallorca in the western Mediterranean (Fig. 1A), caves exist that provide an extraordinary setting for capturing past sea-level changes. The caves formed by the mixing of fresh water and seawater in the coastal phreatic zone (*7*) and contain numerous speleothems (such as stalactites and stalagmites) that formed in early Quaternary time when the caves were air-filled chambers. Throughout the Middle and Late Quaternary, the caves were repeatedly flooded by glacioeustatic sea-level oscillations. The water level of each flooding event was recorded by a distinct encrustation of calcite or aragonite over existing speleothems and along cave walls (Fig. 1B). Similar encrustations form at present in a low-amplitude tide-controlled microenvironment, at or a few centimeters above and below the water table (Fig. 1, C, D, and G). U/Th dating of the outside of these modern encrustations yields present-day ages, whereas subsamples from their interiors yield ages of ~2.8 thousand years ago (ka) (*8*), demonstrating they are indeed "modern" and also that mean sea level has remained stable on Mallorca for the past ~2800 years. We have identified several well-defined encrustation levels below and above the present-day sea level corresponding to older sea-level stands (Fig. 1, E and F), and we used such encrustations to determine relative sea level during MIS 5a.

We collected six speleothem encrustations from five different caves along the eastern and southern coast of Mallorca (Fig. 1A). All the sampled caves in our study are within a horizontal distance of 250 m of the coast; thus, the water table of the caves is, and was in the past, coincident with sea level. The encrustations were sampled from two distinct horizons located at 1.2 to 1.5 and 2.6 m (±5 cm) above present sea level. The errors associated with sample elevations are well within the 50-cm maximum amplitude of water-level oscillations due to barometric tides. Two subsamples were dated from most overgrowths (*9*); the main subsample was extracted from the widest part of the overgrowth, thought to represent the mean sea-level position. When possible, another subsample was milled within 2 to 8 cm above the main one.

Three stages of sea-level encrustations were identified by U/Th ages of 80 to 82 ka, 116 ka, and 121 ka (Table 1). The ages of 116 ka and 121 ka obtained for two encrusted speleothems collected from elevations of ~2.6 m are consistent with previous results for MIS 5e sea level in Mallorca (*1*, *10*) and are also consistent, within a few meters, with many other estimates from around the world of eustatic sea level during MIS 5e. Although we cannot be certain that peak MIS 5e sea level has been captured by our sampled encrustations at 2.6 m, the observation nonetheless suggests that tectonic motion is not a major confounding factor in our reconstruction of MIS 5a sea level, because it is implausible that MIS 5a deposits could be significantly elevated by tectonics while MIS 5e deposits were not. Our results at face value therefore indicate that between ~82 and 80 ka, sea level in Mallorca stood at ~ +1 m relative to present sea level (Table 1 and Fig. 2A).

If interpreted solely as a change in ice-equivalent sea level, our ~ +1 m MIS 5a highstand conflicts with reconstructions from raised coral reefs from uplifting coastlines (such as Haiti, Barbados, and New Guinea), which suggest that MIS 5a eustatic sea level was anywhere from 7 m (one "Greenland equivalent") to 30 m (four "Greenland equivalents") below present sea level (*2*, *3*, *11*, *12*). Lower-than-present sea levels at ~80 ka have also been inferred from submerged speleothems from Grand Bahama Island (*13*) and coral reefs on the Florida Keys (*14*).

Relative sea-level change at a site, however, reflects not only changes in global ice volume but also the response of Earth to changes in surface loading in the form of surface deformation and geoid changes, or glacial isostatic adjustment (GIA) (*3*, *15*). Thus, at any site, and in the absence of tectonic effects, relative sea level in its most simple expression reflects two unknown parameters: GIA and eustacy. GIA has both glacio- and hydro-components (*3*, *15*, *16*). The Mediterranean Sea is an intermediate-field basin, moderately distant from the former major glaciation centers of the Northern Hemisphere (*16*). Thus, the ~1-m elevation of the ~81-ka highstand at Mallorca may plausibly contain a significant effect of GIA associated with Northern Hemisphere ice sheet history. A similar scenario has been proposed for other intermediate-field sites that display evidence for a near-modern MIS 5a sea level (*5*), so as to remain consistent with the far-field estimates of MIS 5a eustatic sea level from Barbados and New Guinea of ~ –10 to –20 m.

Numerical models generally estimate GIA with assumptions about the thickness, distribu-

[1]Department of Geoscience, University of Iowa, 121 Trowbridge Hall, Iowa City, IA 52242, USA. [2]Department of Geology, University of South Florida, 4202 East Fowler Avenue, SCA 528, Tampa, FL 33620, USA; and Department of Geology, Babes-Bolyai University, Emil Racovita Institute of Speleology Cluj, Romania. [3]Departament de Ciències de la Terra, Universitat de les Illes Balears, Carretera Valldemossa km 7.5, Palma de Mallorca, 07122, Spain. [4]Dipartimento di Scienze Geologiche, Università di Roma III, Largo St. Leonardo Murialdo, 1, 00146 Roma, Italy.

*To whom correspondence should be addressed. E-mail: jeffrey-dorale@uiowa.edu (J.A.D.); bonac@cas.usf.edu (B.P.O.). These authors contributed equally to this work.

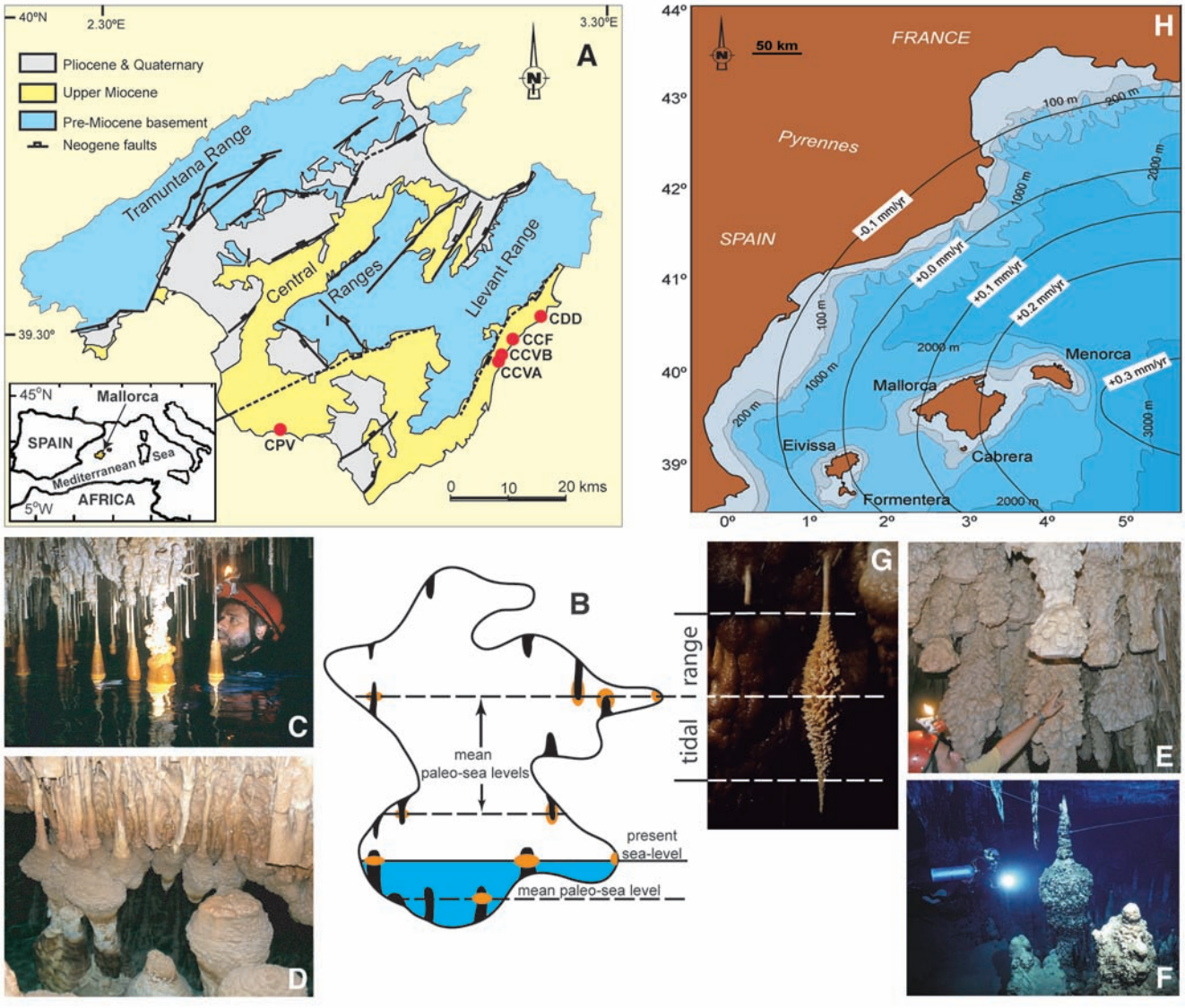

Fig. 1. Encrusted speleothems at various levels in caves from Mallorca. (**A**) Geologic map of Mallorca (*10*) and location of sampled caves (red dots). (**B**) Schematic cross-section through a coastal cave in Mallorca showing multiple carbonate encrustation levels. (**C** and **D**) Present-day and paleo levels of encrusted speleothems related to higher (**E**) and lower (**F**) sea-level stands. (**G**) Typical morphology for tidal range–related carbonate encrustation (size of speleothem, 20 cm). (**H**) Bathymetric map of the western Mediterranean region and the predicted present-day rate of sea-level change due to GIA [adapted from (*15*)].

tion, and duration of former ice loads as well as the viscoelastic properties of Earth. Because eustatic sea level has been relatively stable during the late Holocene (*17*), this is a useful period for comparing the predictions of GIA models and the field evidence of sea-level changes. Some models predict a nearly constant sea-level rise on the order of 0.2 mm/year in the vicinity of Mallorca throughout the late Holocene, due to hydroisostatic subsidence of the basin (*15*, *18*) (Fig. 1H). This equates to 60 cm of sea-level rise over the past 3000 years. But the modern, actively accreting speleothem encrustations from Mallorca (Fig. 1, C and D) show instead that relative sea level has remained stable over the past ~2800 years (*8*). We therefore propose that Mallorca's location in the western Mediterranean may actually be somewhat unusual with regard to GIA. According to the models of (*15*) and (*18*), Mallorca is fairly close to (within 100 km) the predicted zone of neutral GIA to the west (Fig. 1H). Mallorca is also part of a shallow-water shelf extending from the Iberian mainland (Fig. 1H) that would probably have some effect on the hydroisostatic properties of the site, but this detail has probably not been incorporated into GIA models because of their relatively coarse resolution. In any case, the late Holocene field evidence from Mallorca does indeed indicate that the GIA effects of (*15*) and (*18*) have been overestimated for this region, suggesting the possibility that Mallorca occupies a narrow transition zone between regions of emergence and submergence in the Mediterranean basin, where sea level nearly follows the eustatic curve (*19*).

From our data and that of (*10*) and (*20*), we estimate that the MIS 5a sea-level highstand involved very rapid ice melting leading up to the event and had a duration on the order of 4000 years, from ~84 to 80 ka (Fig. 2C). This duration is similar to estimates from Bermuda of ~5000 years (*2*). Specifically at Mallorca, speleothem encrustations record a MIS 5b sea-level height of ~ –20 m at 85.4 ± 0.9 ka and a MIS 5a height of ~ +1 m by 84.2 ± 1.0 ka (*10*). The sea-level drop after the MIS 5a highstand was very rapid as well, because speleothem encrustations record a height of ~ –15 m by ~78.6 ± 0.8 ka (*10*). These rates of sea-level change nominally approach 20 m per thousand years (ky), which is comparable to the meltwater pulses of the last major deglaciation (*21*) and almost 30 times

larger than the largest observed or predicted rates of GIA (*15*). Thus, the MIS 5b/5a/4 sequence at Mallorca demonstrates that very large eustatic changes were involved with the MIS 5a highstand.

We therefore consider the simple interpretation of our data that eustatic sea level during MIS 5a stood around +1 m relative to present sea level, implying less ice on Earth 81,000 years ago than today. Although this interpretation conflicts with the generally accepted eustatic sea-level curve based on the far-field sites of Barbados and New Guinea, it is consistent with a number of other estimates from around the world, including those from the Bahamas, the U.S. Atlantic Coastal Plain, Bermuda, Cayman Islands, and California (*4*, *6*, *22*–*26*) (Fig. 2B). We considered the simple fact that this geographically diverse suite of sites spans a wide range of presumed isostatic states, yet the suite consistently indicates a late MIS 5a highstand of ~ +0 to 3 m (Fig. 2B). Bermuda and Mallorca, for example, are both tectonically stable, and both have MIS 5e/5a estimates of 2 to 3 and 1 to 2 m above modern sea level, respectively; whereas MIS 5e/5a estimates from Barbados are ~ +5 m and ~ –18 m (*2*). Any appeal to GIA to account for these discrepancies must somehow take into account the unlikely outcome that different ice centers on different continents (Laurentide versus Fennoscandian) would generate the virtually

Table 1. Sample information and U/Th data. Errors are 2σ of the mean and are based on the analytical precision. m apsl, meters above present sea level; ppm, parts per million; AR, activity ratio.

Cave	Sample code	Elevation (m apsl)	U (ppm)	$^{234}U/^{238}U$ (initial)	$^{234}U/^{238}U$ (measured)	$^{230}Th/^{232}Th$ AR	$^{230}Th/^{234}U$ AR	Age (ka) ±2σ	
Cova de Cala Varques A	CCVA-1	1.25	0.110 ± 0.022	1.476 ± 0.086	1.377 ± 0.069	9077	0.5450 ± 0.0021	81.95	±0.56
	CCVA-2	1.30	0.121 ± 0.018	1.478 ± 0.069	1.379 ± 0.055	5599	0.5440 ± 0.0020	81.66	±0.45
Cova del Dimoni	CDD-1	1.48	1.191 ± 0.019	1.223 ± 0.038	1.178 ± 0.003	18814	0.5297 ± 0.0039	80.44	±0.61
	CDD-2	1.45	1.186 ± 0.018	1.222 ± 0.034	1.177 ± 0.027	17160	0.5298 ± 0.0028	80.65	±0.46
Cova de Cala Varques B	CCVB	1.32	0.101 ± 0.021	1.473 ± 0.021	1.376 ± 0.017	418	0.5413 ± 0.0046	80.78	±0.96
Cova de Cala Falcó	CCF-1	1.57	0.208 ± 0.023	2.397 ± 0.011	2.113 ± 0.009	2410	0.5510 ± 0.0023	80.43	±0.48
	CCF-2	1.53	0.202 ± 0.021	2.431 ± 0.015	2.137 ± 0.012	990	0.5563 ± 0.0023	81.10	±0.49
Cova des Pas de Vallgornera	CPV-1	1.60	0.156 ± 0.030	1.408 ± 0.024	1.325 ± 0.019	31537	0.5350 ± 0.0028	80.09	±0.48
	CPV-2	1.52	0.144 ± 0.028	1.413 ± 0.026	1.329 ± 0.021	34757	0.5361 ± 0.0019	80.12	±0.45
	CPV-B8	1.52	0.119 ± 0.018	1.492 ± 0.020	1.391 ± 0.016	1812	0.5410 ± 0.0022	80.97	±0.48
	CPV-B6	2.60	0.108 ± 0.020	1.198 ± 0.018	1.141 ± 0.013	1892	0.6830 ± 0.0027	120.60	±0.89
	CPV-B9	2.60	0.122 ± 0.014	1.240 ± 0.017	1.173 ± 0.012	1151	0.6710 ± 0.0019	116.20	±0.61

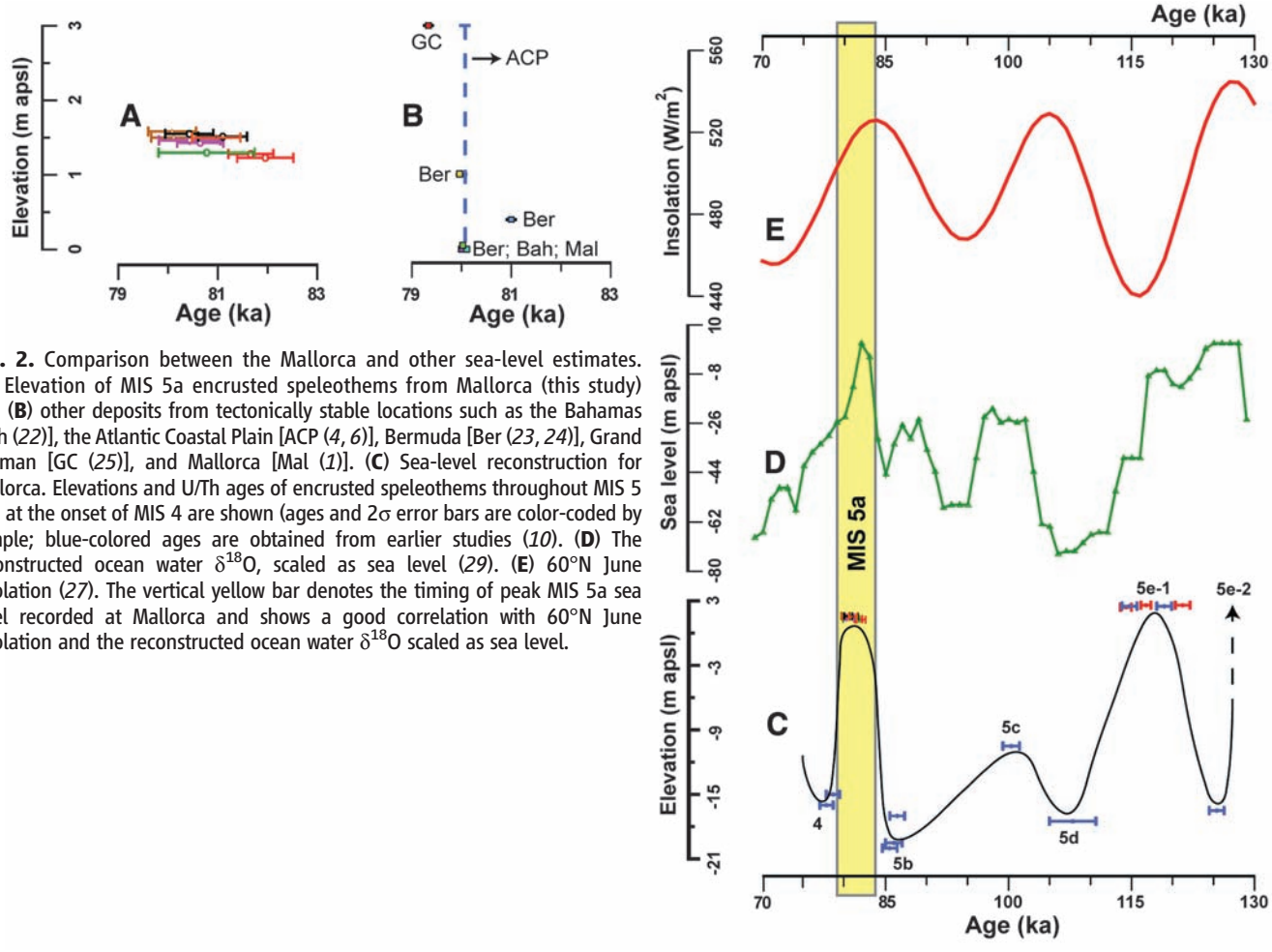

Fig. 2. Comparison between the Mallorca and other sea-level estimates. (**A**) Elevation of MIS 5a encrusted speleothems from Mallorca (this study) and (**B**) other deposits from tectonically stable locations such as the Bahamas [Bah (*22*)], the Atlantic Coastal Plain [ACP (*4*, *6*)], Bermuda [Ber (*23*, *24*)], Grand Cayman [GC (*25*)], and Mallorca [Mal (*1*)]. (**C**) Sea-level reconstruction for Mallorca. Elevations and U/Th ages of encrusted speleothems throughout MIS 5 and at the onset of MIS 4 are shown (ages and 2σ error bars are color-coded by sample; blue-colored ages are obtained from earlier studies (*10*). (**D**) The reconstructed ocean water $\delta^{18}O$, scaled as sea level (*29*). (**E**) 60°N June insolation (*27*). The vertical yellow bar denotes the timing of peak MIS 5a sea level recorded at Mallorca and shows a good correlation with 60°N June insolation and the reconstructed ocean water $\delta^{18}O$ scaled as sea level.

identical MIS 5e/5a relative sea-level histories of tectonically stable Bermuda and Mallorca. The very rapid onset and relatively brief nature of the MIS 5a highstand may have plausibly generated lags between the timing of sea-level changes and the timing of coral reef growth, and may provide a partial explanation as to why reefs on Barbados and New Guinea do not record a comparable eustatic height for this event. This and other factors that could be part of the apparent discrepancy are discussed in (*9*).

The suggestion that MIS 5a sea level was slightly higher than at present and only slightly lower than the MIS 5e sea level implies that most of the ice built up during MIS 5b would have melted during the onset of MIS 5a. The ~84- to 80-ka timing of this highstand closely matches the June 60°N insolation peak at ~84 ka (Fig. 2E), a pattern that is consistent with the Milankovitch model. In fact, June insolation at 60°N was higher at ~84 ka than that at 11 ka (*27*), and field studies in the Baffin Island region suggest the complete melting of the Laurentide Ice Sheet around 80 ka (*28*). Finally, we find additional, independent support for a near-modern eustatic MIS 5a highstand when we consider the indirect sea-level estimate of (*29*) inferred from a Pacific benthic $\delta^{18}O$ record, the Vostok atmospheric $\delta^{18}O$ record, and certain assumptions about the Dole effect on deep-water temperatures (Fig. 2D). The premise of the approach of (*29*) is that the deep-sea $\delta^{18}O$ record does not capture the true magnitude of eustatic sea-level change, because the $\delta^{18}O$ signal is partially controlled by temperature.

Because of its relation to continental ice volume, an accurate Quaternary sea-level curve has been a long-term goal of scientists interested in ice-age cycles and their causes. Ice-age theory has long assumed gradual ice buildup and more rapid ice melting in the generally accepted model of the ~100-ky cycle of glaciation. Instead, the emerging body of evidence suggests that both melting and accumulation can be very rapid during discrete intervals of time when specific conditions prevail. Furthermore, the 100-ky model of glaciation has always faced the problem that although the deep-sea $\delta^{18}O$ record is dominated by a 100-ky cycle, northern high-latitude summer insolation has negligible power in this band. Our data from Mallorca and data from other sites around the world indicate the possibility that eustatic sea level was near modern levels at ~80 ka. If this is true, the 100-ky cycle so universally accepted as the main rhythm of the Middle and Late Quaternary glaciations, in fact, applies rather poorly to ice growth and decay, but much better to carbon dioxide, methane, and temperatures recorded by polar ice (*30*).

References and Notes

1. P. J. Hearty, *Quat. Sci. Rev.* **6**, 245 (1987).
2. C. D. Gallup, R. L. Edwards, R. G. Johnson, *Science* **263**, 796 (1994).
3. K. Lambeck, J. Chappell, *Science* **292**, 679 (2001).
4. D. R. Muhs, K. R. Simmons, B. Steinke, *Quat. Sci. Rev.* **21**, 1355 (2002).
5. E. K. Potter, K. Lambeck, *Earth Planet. Sci. Lett.* **217**, 171 (2003).
6. J. F. Wehmiller *et al.*, *Quaternary Int.* **120**, 3 (2004).
7. J. Ginés, *Endins* **20**, 71 (1995).
8. P. Tuccimei *et al.*, *Earth Surf. Process. Landf.* **35**, (2010).
9. Materials, methods, and additional discussion are available as supporting material on *Science* Online.
10. P. Tuccimei *et al.*, *Z. Geomorphol.* **50**, 1 (2006).
11. R. E. Dodge, R. G. Fairbanks, L. K. Benninger, F. Maurrasse, *Science* **219**, 1423 (1983).
12. T. M. Esat, M. T. McCulloch, J. Chappell, B. Pillans, A. Omura, *Science* **283**, 197 (1999).
13. W. X. Li *et al.*, *Nature* **339**, 534 (1989).
14. M. A. Toscano, J. Lundberg, *Quat. Sci. Rev.* **18**, 753 (1999).
15. J. X. Mitrovica, G. A. Milne, *Quat. Sci. Rev.* **21**, 2179 (2002).
16. P. A. Pirazzoli, *Quat. Sci. Rev.* **24**, 1989 (2005).
17. K. Lambeck, M. Azidei, F. Antonioli, A. Benini, A. Esposito, *Earth Planet. Sci. Lett.* **224**, 563 (2004).
18. W. R. Peltier, *Annu. Rev. Earth Planet. Sci.* **32**, 111 (2004).
19. P. Stocchi, G. Spada, *Ann. Geophys.* **50**, 741 (2007).
20. E. J. Hodge, D. A. Richards, P. L. Smart, A. Ginés, D. P. Mattey, *J. Quat. Sci.* **23**, 713 (2008).
21. R. L. Edwards *et al.*, *Science* **260**, 962 (1993).
22. P. J. Hearty, *Quat. Sci. Rev.* **17**, 333 (1998).
23. K. R. Ludwig, D. R. Muhs, K. R. Simmons, R. B. Halley, E. A. Shinn, *Geology* **24**, 211 (1996).
24. H. L. Vacher, P. Hearty, *Quat. Sci. Rev.* **8**, 159 (1989).
25. M. K. Coyne, B. Jones, D. Ford, *Quat. Sci. Rev.* **26**, 536 (2007).
26. D. R. Muhs, J. F. Wehmiller, K. R. Simmons, L. L. York, in *The Quaternary Period in the United States*, A. R. Gillespie, S. C. Porter, B. F. Atwater, Eds. (Elsevier, Amsterdam, 2004), pp. 147–183.
27. A. Berger, M. F. Loutre, *Quat. Sci. Rev.* **10**, 297 (1991).
28. G. H. Miller *et al.*, *Quat. Sci. Rev.* **18**, 789 (1999).
29. N. J. Shackleton, *Science* **289**, 1897 (2000).
30. J. R. Toggweiler, *Paleoceanography* **23**, PA2211 (2008).

31. This material is based on work supported by NSF (grant OISE-0826667 to B.P.O. and J.A.D.), the University of South Florida (grant R058889) to B.P.O., and the MICINN-FEDER Projects CGL2006-11242-C03-01 and CGL2009-07392 of the Spanish Government to J.J.F. We thank L. Vacher, V. Polyak, and E. A. Bettis III for stimulating discussions, three anonymous reviewers for insightful criticism that considerably improved the manuscript, and F. Gràcia and K. Downey for some of the pictures.

Supporting Online Material

www.sciencemag.org/cgi/content/full/327/5967/860/DC1
Materials and Methods
SOM Text
References

9 September 2009; accepted 7 January 2010
10.1126/science.1181725

A Genetic Variant BDNF Polymorphism Alters Extinction Learning in Both Mouse and Human

Fatima Soliman,[1,2]* Charles E. Glatt,[2] Kevin G. Bath,[2] Liat Levita,[1,2] Rebecca M. Jones,[1,2] Siobhan S. Pattwell,[2] Deqiang Jing,[2] Nim Tottenham,[1,2] Dima Amso,[1,2] Leah H. Somerville,[1,2] Henning U. Voss,[3] Gary Glover,[4] Douglas J. Ballon,[3] Conor Liston,[1,2] Theresa Teslovich,[1,2] Tracey Van Kempen,[1,2] Francis S. Lee,[2]* B. J. Casey[1,2]*

Mouse models are useful for studying genes involved in behavior, but whether they are relevant to human behavior is unclear. Here, we identified parallel phenotypes in mice and humans resulting from a common single-nucleotide polymorphism in the brain-derived neurotrophic factor (BDNF) gene, which is involved in anxiety-related behavior. An inbred genetic knock-in mouse strain expressing the variant BDNF recapitulated the phenotypic effects of the human polymorphism. Both were impaired in extinguishing a conditioned fear response, which was paralleled by atypical frontoamygdala activity in humans. Thus, this variant BDNF allele may play a role in anxiety disorders showing impaired learning of cues that signal safety versus threat and in the efficacy of treatments that rely on extinction mechanisms, such as exposure therapy.

Genetically modified mice provide useful model systems for testing the role of candidate genes in behavior. The extent to which such genetic manipulations in the mouse and the resulting phenotype can be translated across species, from mouse to human, is less clear. In this report, we focused on identifying biologically valid phenotypes across species. We utilized a common single-nucleotide polymorphism (SNP) in the brain-derived neurotrophic factor (BDNF) gene that leads to a valine (Val) to methionine (Met) substitution at codon 66 (Val66Met). In an inbred genetic knock-in mouse strain that expresses the variant BDNF allele to recapitulate the specific phenotypic properties of the human polymorphism in vivo, we found the BDNF Val66Met genotype was associated with treatment-resistant forms of anxiety-like behavior (*1*). The objective of this study was to test if the Val66Met genotype could affect extinction learning in our mouse model and whether such findings could be generalized to human populations.

[1]The Sackler Institute for Developmental Psychobiology, Weill Cornell Medical College, New York, NY 10065, USA. [2]Department of Psychiatry, Weill Cornell Medical College, New York, NY 10065, USA. [3]Citigroup Biomedical Imaging Center, Department of Radiology, Weill Cornell Medical College, New York, NY 10065, USA. [4]Lucas Center for Imaging, Department of Radiology, Stanford University, Stanford, CA 94305, USA.

*To whom correspondence should be addressed. E-mail: fas2002@med.cornell.edu (F.S.) or fslee@med.cornell.edu (F.S.L.) or bjc2002@med.cornell.edu (B.J.C.)